Journal of NeuroVirology, 15: 458–464, 2009

ISSN 1355-0284 print / 1538-2443 online
DOI: 10.3109/13550280903473460

informa
healthcare

Short communication

Advanced tracing tools: functional neuronal expression of virally encoded fluorescent calcium indicator proteins

Markus Rothermel,[1,3] Daniela Brunert,[1] Barbara G. Klupp,[2] Matthias Luebbert,[1] Thomas C. Mettenleiter,[2] and Hanns Hatt[1]

[1]*Lehrstuhl für Zellphysiologie, Ruhr-Universität, Bochum, Germany;* [2]*Friedrich-Loeffler-Institut, Bundesforschungsinstitut für Tiergesundheit, Insel Riems, Germany; and* [3]*Graduiertenkolleg GRK736* "*Development and Plasticity of the Nervous System: Molecular, Synaptic and Cellular Mechanisms,*" *Ruhr-Universität, Bochum, Germany*

Pseudorabies virus (PrV) strains such as PrV-Bartha and its marker protein-expressing variants have been used in numerous studies as retrograde trans-neuronal tracing tools, defining the synaptic organization of mammalian neuronal circuits. However, the possibilities for functional examination of virus-infected neurons are limited to electrophysiological approaches or bulk loading strategies using calcium-sensitive dyes. Herein we report the generation and functional characterization of three PrV-Bartha–derived recombinant virus mutants that express different fluorescent calcium indicator proteins (FCIPs). All three generated virus recombinants are able to infect murine trigeminal neurons and express the corresponding FCIP (GCaMP2, camgaroo-2, or inverse pericam). Functionality of these virally expressed constructs was verified by using confocal Ca-imaging technologies. These FCIP-expressing virus recombinants provide a new tool for the functional analysis of whole circuits of synaptically connected neurons *in vitro* and *in vivo.* *Journal of NeuroVirology* (2010) **15**, 458–464.

Keywords: pseudorabies virus; fluorescent calcium indicator proteins; mice; trigeminal system; confocal calcium imaging

In recent years research has increasingly focused on the exploration of neuronal networks. For decryption of neuronal network information processing, it is essential to measure simultaneously neuronal activity at multiple locations at a high temporal and spatial resolution. Originally, this has been achieved by electrophysiological recordings. However, patch clamp techniques are limited to simultaneous measurements from only a restricted number of neurons, whereas most multi-microelectrode

Address correspondence to Dr. Markus Rothermel, Lehrstuhl für Zellphysiologie, Fakultät für Biologie und Biotechnologie, Ruhr-Universität, Universitätsstrasse 150, D-44780 Bochum, Germany. E-mail: Markus.Rothermel@rub.de

The present address of Markus Rothermel is Department of Biology, Boston University, Boston, USA.

The present address of Daniela Brunert is Center for Smell and Taste, University of Florida, Gainesville, USA

This work was supported by the Deutsche Forschungsgemeinschaft (DFG) (Graduiertenkolleg 736 "Development and Plasticity of the Nervous System: Molecular, Synaptic and Cellular Mechanisms," University of Bochum, Bochum, Germany; research grant DFG Me 854/9-2 to T.C.M.) and by the Ruhr-University Research School funded by the DFG in the framework of the Excellence Initiative and the Wilhelm und Günter Esser Stiftung (Ruhr-University Bochum).

The authors thank Harald Bartel for his technical support with equipping the imaging setup and Diana Werner for support with generation of viral recombinants. The FCIP construct inverse pericam was kindly provided by Dr. A. Miyawaki (Laboratory for Cell Function and Dynamics, Advanced Technology Development Center, Brain Science Institute, Institute of Physical and Chemical Research [RIKEN], Saitama, Japan). The FCIP construct GCaMP2 was kindly provided by Dr. J. Nakai (Laboratory for Memory and Learning, RIKEN Brain Science Institute). The FCIP construct camgaroo-2 was kindly provided by Dr. O. Griesbeck (AG Zelluläre Dynamik, Max-Planck-Institut für Neurobiologie, Martinsried, Germany) and Dr. R. Y. Tsien (Department of Pharmacology and Howard Hughes Medical Institute, University of California at San Diego, La Jolla, California, USA).

Received 27 May 2009; revised 20 August 2009; accepted 28 September 2009.

arrays suffer from low spatial resolution of the recorded field potentials. Therefore many studies tried to overcome these problems by using opto-physiological approaches.

Calcium imaging represents one of the most advantageous imaging approaches, combining an acceptable temporal and excellent spatial resolution with high fractional changes of fluorescence intensity.

Despite the advantages of calcium-sensitive dyes, cell type–specific labeling cannot be achieved using bulk loading approaches, which result in high background fluorescence values and decreased signal to noise ratios. Additionally, not all adult neuronal tissues take up the dyes in sufficient amounts. A significant improvement in this respect was the development of fluorescent calcium indicator proteins (FCIPs). Several FCIPs have been described in recent years, e.g., pericam (Nagai *et al.* 2001), camgaroo (Baird *et al.* 1999), or GCaMP (Nakai *et al.* 2001). All these constructs are direct (nonratiometric) Ca^{2+} probes composed of a single fluorescent protein. GCaMPs and pericams were generated from the circularly permuted green and yellow fluorescent proteins, respectively (Nakai *et al.* 2001; Nagai *et al.* 2001). The C-terminus of the chromophore was connected to calmodulin and the N-terminus to its target peptide, M13. Despite this common structural design, dramatic changes in Ca^{2+} responses were observed even between constructs of the same FCIP family. Thus, mutations of amino acids adjacent to the chromophore led to different types of pericams. So-called "flash pericam" became brighter with an increase in intracellular Ca^{2+}, whereas "inverse pericam" dimmed (Nagai *et al.* 2001). To obtain camgaroo-1, calmodulin has been inserted in the middle of the circularly permuted yellow fluorescent protein (Baird *et al.* 1999). Camgaroo-2 was subsequently generated by a random mutation in camgaroo-1 (Griesbeck *et al.* 2001). Apart from inverse pericam, the described indicators increase their fluorescence with a raise in calcium concentration.

Using appropriate promoters these calcium sensors can be expressed in specific cell types, thereby dramatically increasing signal to noise ratios especially in tissue slices and *in vivo* preparations. These advantages led to the creation of transgenic animals, including worms (Kerr *et al.* 2000; Suzuki *et al.* 2003), fruitflies (Fiala *et al.* 2002; Reiff *et al.* 2002; Liu *et al.* 2003; Wang *et al.* 2003; Yu *et al.* 2003), zebrafish (Higashijima *et al.* 2003), and mice (Ji *et al.* 2004; Hasan *et al.* 2004), manipulated to express these proteins in selected tissues.

However, construction of transgenic animals, in particular mice, is slow and expensive because each cell or tissue system of interest requires a separate transgenic line. Thus, for a fast and reliable introduction of FCIPs into various mammalian cells, a viral vector represents the perfect tool for the functional analysis of whole circuits of synaptically connected neurons *in vitro* and *in vivo.* Virally mediated expression of these constructs would therefore have a broad field of application in the neurosciences.

Here, we report the generation of viral vectors expressing three different functional calcium indicators. As vector, the neurotropic alphaherpesvirus pseudorabies virus (PrV) strain Bartha was chosen, since this virus has been established as a "live-cell" tracing tool allowing a functional analysis of infected neurons (Damann *et al.* 2006).

Three different FCIPs were utilized: inverse pericam (Nagai *et al.* 2001), camgaroo-2 (Griesbeck *et al.* 2001), and GCaMP2 (Diez-Garcia *et al.* 2005). These FCIPs were selected for their respective molecular weight and their reported magnitude of stimulus-induced fluorescence changes.

Functional expression of FCIP plasmid constructs was verified in transfected HEK 293 cells. All constructs showed a robust expression and a homogeneous cytosolic fluorescence (data not shown).

For calcium imaging experiments, cells were continuously perfused with Ringer's solution (450 to 500 μl/min) using a specialized microcapillary system. Perfusion was switched transiently to stimulus or control (Ringer's solution) application thereby maintaining the continuous liquid stream.

Functionality of the expressed constructs was tested by stimulating the cells with ATP (300 μM), which resulted in fluorescence changes for all of the three tested FCIPs. Relative fluorescence changes ($\Delta F/F$) of up to −35% (mean −15.3% ± 0.55% [SEM]; n = 200 cells) for inverse pericam, up to 23.9% (mean 9.5% ± 0.97% [SEM]; n = 29 cells) for camgaroo-2, and up to 166.7% (mean 54.4% ± 4.1% [SEM]; n = 96 cells) for GCaMP2 could be observed (number of cells obtained from at least four independent experiments; cells were typically measured 1 to 2 days after transfection).

Because functionality of all calcium-sensitive proteins could be confirmed, three different PrV-Bartha recombinants containing the respective constructs were generated. Plasmids pcDNA-camgaroo-2 (kindly provided by Dr. O. Griesbeck and Dr. R. Y. Tsien) and pcDNA-inverse pericam (kindly provided by Dr. A. Miyawaki) were digested with NruI and PvuII. The resulting 2.2-kb fragment comprising the immediate-early 1 promoter/enhancer region of human cytomegalovirus (HCMV) and the 1.2-kb camgaroo-2 or inverse pericam open reading frames were cloned into vector pU6.3, containing a 6.3-kb SphI fragment of genomic PrV strain Kaplan DNA comprising the gG gene region. To this end, vector pU6.3 was cleaved with BamHI, thereby removing an approximately 200-bp fragment of the gG gene region (Figure 1A,B). Vector and insert fragments were treated with Klenow polymerase to generate blunt ends and ligated giving rise to pU6.3-cam2 or pU6.3-inverse pericam, respectively. The HCMV immediate-early promoter/enhancer-GCaMP2

expression cassette was derived from plasmid pEGFP-N1-GCaMP2 (kindly provided by Dr. J. Nakai) after cleavage with AseI and AflII. The resulting 2.2-kb fragment was cloned into pU6.3 as described above.

These plasmids were used for cotransfections with PrV genomic DNA of the attenuated PrV strain Bartha K61 (Bartha, 1961) into RK13 rabbit kidney cells. Transfection progeny was screened for autofluorescent plaques, which were plaque purified until homogeneity. One single plaque isolate each, designated as PrV-Bartha_Cam2 (for camgaroo-2), PrV-Bartha_IP (for inverse pericam), and PrV-Bartha_GCaMP2 (for GCaMP2), was chosen randomly, propagated on pig kidney (PSEK) cells and used for further studies.

Correct insertion of FCIP genes was verified by restriction enzyme digest and Southern blotting. To this end, recombinant virus DNA was isolated from infected cell lysates, digested with KpnI, blotted onto nitrocellulose, and probed with radioactively labeled fragments (Figure S1). In RK13 cells, the virus recombinants expressing the FCIP constructs replicated with kinetics comparable to the parental strain PrV Bartha (data not shown).

An *ex in vivo* whole-mount preparation of the base of the skull was used for the identification of infected cells in the trigeminal ganglion (Figure 1C). No differences in the kinetics of viral neuroinvasion into trigeminal ganglion neurons after unilateral intranasal inoculation of mice were observed when comparing the newly constructed mutant viruses with previously used PrV-Bartha recombinants (Figure 1D).

For functional analysis of the virally encoded FCIPs, primary murine neuronal trigeminal cell cultures (Spehr *et al.* 2004) were infected *in vitro* with the different viral constructs. Infection was performed as described previously (Damann *et al.* 2006). Twenty-four hours after plating, neuronal cell cultures were infected at a multiplicity of infection of 100 plaque-forming units (PFU)/cell and incubated for 1 h at 37°C. Afterwards, cells were washed 2 times with growth medium containing 10% fetal bovine serum to remove unabsorbed virus. Infected cultures were incubated in growth medium containing the direct noncompetitive viral DNA-polymerase inhibitor foscarnet (Helgstrand *et al.* 1978) (FO, Fluka) (400 μg/ml) at 37°C.

Each of the generated virus recombinants showed a robust FCIP expression in infected trigeminal neurons, indicated by a basic fluorescence that was homogeneously distributed within the cytosol of the respective cells (Figure 2A–C). In phase-contrast light microscopy, the general appearance of infected neuronal cell bodies did not differ from noninfected neurons; therefore, infected cells could only be identified using fluorescence microscopy. Marker protein–expressing cells displayed typical trigeminal ganglion neuron morphology with spherical and pseudounipolar shape and long processes. Emission spectra of infected cells displayed the construct specific maxima, arguing for a correct virally mediated FCIP expression (data not shown).

Functionality of virally expressed FCIPs was tested by neuronal depolarization using 45 mM potassium chloride. Neuronal stimulation resulted in significant changes in fluorescence for all of the three tested virally expressed FCIPs. Fractional changes in fluorescence intensity were up to −31.5% (mean −18.9% ± 1.4% [SEM]; n = 21 neurons) for PrV-Bartha_IP, up to 21.9% (mean 16% ± 1.5% [SEM]; n = 8 neurons) for PrV-Bartha_Cam2, and up to 133.6% (mean 79.1% ± 5.9% [SEM]; n = 33 neurons) for PrV-Bartha_GCaMP2 (Figure 2D) (number of cells obtained from at least four independent experiments; cells were typically measured 1 to 2 days after infection).

These results demonstrate that all constructed virus recombinants functionally express the respective calcium indicator protein in infected cells. Moreover, PrV-Bartha's innate neurotropic tracing abilities were preserved.

The chosen stimulus, 45 mM potassium chloride, should strongly depolarize the neurons and, thus, elicit a maximum calcium response, tapping the full potential of the FCIPs. Virally mediated expression does not appear to influence FCIP functionality, since fractional changes in fluorescence intensity of virally expressed FCIPs were similar to those of FCIPs transiently expressed after transfection into HEK 293 cells. Comparison between the different virally expressed FCIPs revealed that PrV-Bartha_GCaMP2 showed the highest fractional changes in fluorescence intensity, whereas PrV-Bartha_IP and PrV-Bartha_Cam2 elicited lesser fractional changes, though PrV-Bartha_IP produced a better signal to noise ratio.

Camgaroo-2 has been described to produce fractional changes in fluorescence intensity of up to 170% (Hasan *et al.* 2004). In our work, we do not reach equally high fractional changes in neurons for that FCIP. However, a viral effect on FCIP expression is unlikely, since the transfected construct in HEK 293 cells also never elicited more than 24% fractional changes in fluorescence intensity. Other studies also demonstrated a similar low Ca^{2+}-sensitivity for camgaroo-2: whereas inverse pericam and GCaMP2 have been reported suitable for detecting calcium transients that accompany single action potentials, at least 8 to 10 spikes were necessary to trigger a reliable fluorescence signal in case of camgaroo-2 (Meyer zum Alten Borgloh *et al.* 2006).

Because whole-cell patch-clamp recordings of cultured trigeminal neurons revealed a significant reduction of spike rate to repetitive potassium chloride stimulation (mean spike rate first application 7.9 ± 1.9 [SEM], n = 19; mean spike rate second application 6.4 ± 1.8 [SEM], n = 17; paired

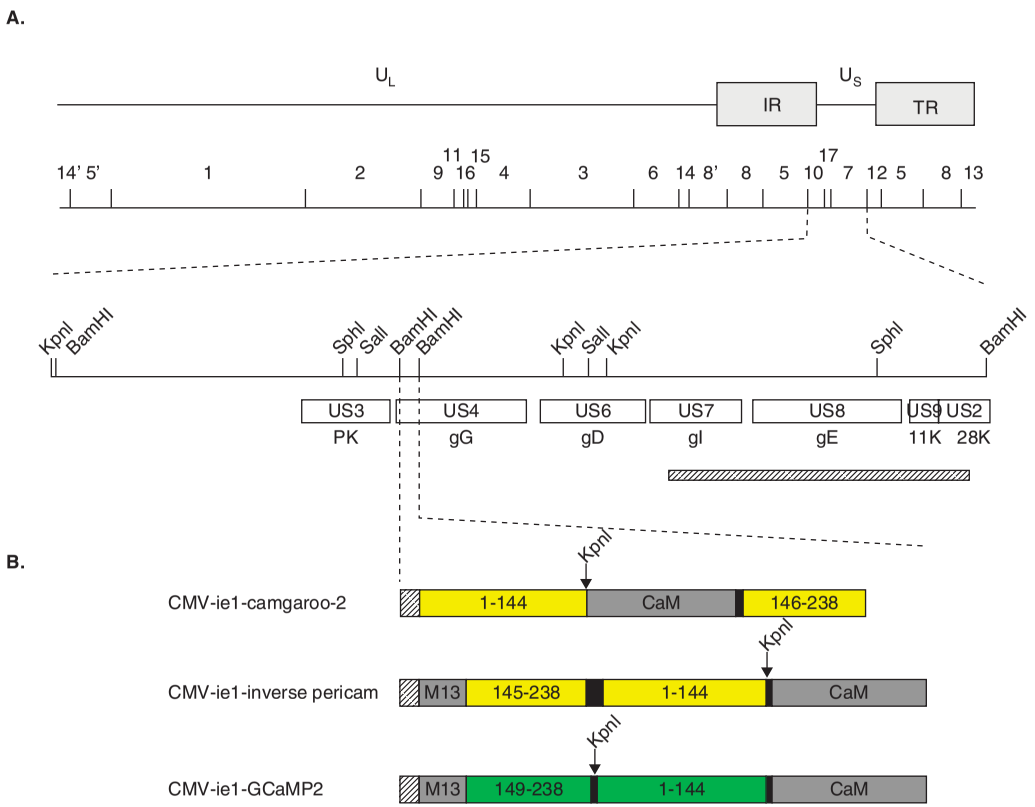

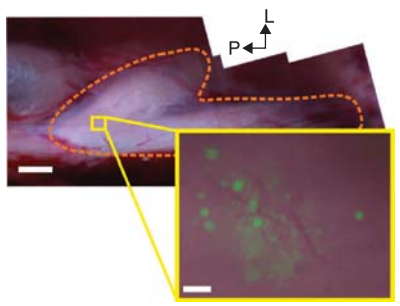

D.

	20 hpi ipsilateral	20 hpi contralateral
PrV-B80	-	-
PrV-Bartha_IP	-	-
PrV-Bartha_Cam2	-	-
PrV-Bartha_GCaMP2	-	-

	40 hpi ipsilateral	40 hpi contralateral
PrV-B80	+	-
PrV-Bartha_IP	+	-
PrV-Bartha_Cam2	+	-
PrV-Bartha_GCaMP2	+	-

	60 hpi ipsilateral	60 hpi contralateral
PrV-B80	++	+
PrV-Bartha_IP	++	+
PrV-Bartha_Cam2	++	+
PrV-Bartha_GCaMP2	++	+

Figure 1. Construction and functional tests of PrV-Bartha strains expressing different fluorescent calcium indicator proteins. (A) Genomic map of the PrV-Bartha strain used in this study. *Top:* Schematic diagram of the wild-type PrV genome with the unique long region (U_L) and the unique short region (U_S), which is bracketed by inverted repeats (IR and TR). Location of BamHI restriction sites are given below. The region used for insertion of the FCIP constructs is shown enlarged at the bottom. The region contains genes encoding a protein kinase (PK; US3), glycoproteins (g)G (US4), gD (US6), gI (US7), gE (US8), and proteins designated as 11K (US9) and 28K (US2). The hatched box indicates the large deletion of sequences in the attenuated PrV-Bartha compared to the wild-type strain PrV-Kaplan. **(B)** Fluorescent calcium indicator proteins used in this study. The camgaroo-2 and inverse pericam constructs are derived from EYFP (indicated in yellow), whereas the GCaMP2 contains the EGFP sequences (green). M13 (myosin light chain kinase) and CaM (calmodulin) are shown in grey and the linker sequences in black. The hatched box indicates the enhancer/promoter region of the human cytomegalovirus immediate early 1 gene (schematic drawings of FCIP constructs adapted from Hasan *et al.* 2004 and Tallini *et al.* 2006). **(C)** Identification of infected cells in the trigeminal ganglion. *Ex in vivo* whole-mount preparation of the base of the skull showing the exposed trigeminal ganglia of an intranasally PrV-Bartha_GCaMP2–infected animal sacrificed 48 h post infection. The trigeminal ganglion is outlined (orange dotted line). The yellow square points to an area where large amounts of infected cells were detected. Fewer infected cells could also be seen at different locations. No differences in the location of infected cells could be observed comparing the three different viral constructs used in this study. Scale bar, 1 mm; P, posterior; L, lateral. Insert: Fluorescence image showing traced nasal trigeminal neurons; scale bar, 40 µm. **(D)** Kinetic of viral neuroinvasion. The PrV-Bartha strains were unilaterally inoculated into one nasal cavity. At 20, 40, and 60 h post infection (hpi), whole-mount preparation of the trigeminal ganglia were analyzed for marker protein expression (−: no cells; +: <20 cells; ++: >20 cells).

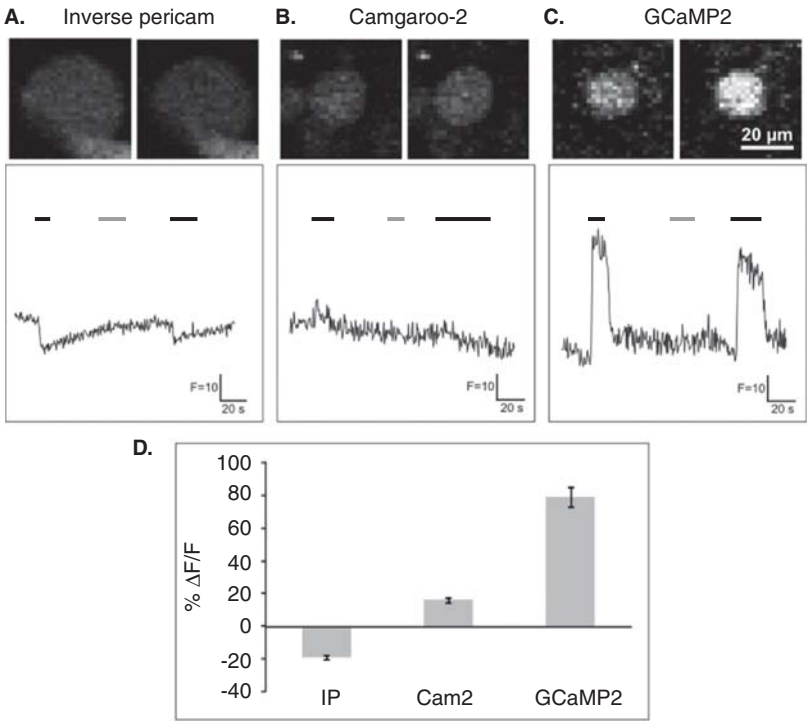

Figure 2. Virally mediated functional FCIP expression in trigeminal neurons. (**A–C**) Trigeminal neurons expressing the virally encoded FCIPs inverse pericam (**A**), camgaroo-2 (**B**), or GCaMP2 (**C**) were imaged by confocal microscopy. *Top*: Resting fluorescence (left) and fluorescence after neuronal depolarisation (right). *Bottom*: representative FCIP responses of stimulated trigeminal neurons. Fluorescence changes were recorded from depicted cell somata (top row, F = fluorescence in arbitrary units). Cells were continuously perfused with Ringer's solution (450–500 µl/min), and perfusion was switched to stimulus application (45 mM potassium chloride; black solid line) or control application (Ringer's solution; grey solid line) to transiently superfuse the cells; scale bar, 20 µm. (**D**) Quantification of FCIP signal amplitudes in trigeminal neurons. Averaged fractional fluorescence changes of virally expressed FCIPs (ΔF/F). Bars represent mean ΔF/F; error bars = SEM.

Student's *t*-test, $p < .05$), differences in response amplitudes to first and second stimulation observed for all FCIP constructs are likely attributable to intrinsic desensitization features of trigeminal neurons.

Several compelling features of neurotropic PrV make it a highly appropriate tool for functional examinations of neuronal networks:

(1) The utility of PrV recombinants as "live-cell" tracing tool allowing a functional analysis of identified neurons has been demonstrated in recent studies (Irnaten *et al*. 2001; Damann *et al*. 2006; Rothermel *et al*. 2007). A main argument against the application of viral tracers for functional investigations has been the possibility that viral infection itself could alter cell physiology. For example, recordings of superior cervical ganglion neurons infected with wild-type PrV-Kaplan or -Bartha strains revealed Kaplan-infected neurons fire spontaneously and continuously, in contrast to silent Bartha-infected or noninfected control neurons (McCarthy *et al*. 2007), all grown under conventional culture conditions. Experiments in our laboratory were performed in the presence of the antiviral drug foscarnet because a detailed electrophysiological characterization of PrV-Bartha– (Damann *et al*. 2006) or PrV-Kaplan– (Rothermel *et al*. 2007) infected trigeminal neurons revealed that compared to infected cells grown with conventional culture medium, infected neurons treated with foscarnet showed unaltered neuronal physiology. In the present study, the fractional fluorescence intensity changes of the virally expressed FCIP constructs could only be observed under foscarnet treatment. Because without foscarnet treatment we observed reduced numbers of infected cells 2 days post infection and the remaining infected cells exerted higher (GCaMP2 and camgaroo-2) or lower (inverse pericam) fluorescence baselines than treated cell, indicating abnormally high intracellular calcium levels, we assume that

this lack of responsiveness may be attributed to a severe damage of untreated cells after infection. Foscarnet can be administered systemically (e.g. intraperitoneally; Alenius *et al*. 1978) so it is also suitable for *in vivo* applications.

(2) PrV has the property to spread exclusively within synaptically connected neurons, which has been exploited in numerous tracing studies. PrV-Bartha, an attenuated live-vaccine strain, proved to be particularly appropriate for this purpose because of its reduced virulence and specific transneuronal spread in the retrograde direction of information processing (Enquist, 2002).

(3) PrV has a broad host spectrum, providing the opportunity of transferring the tracing approach to different model organisms using the same viral constructs. In accordance with that, preliminary experiments performed on rat trigeminal neurons *in vitro* infected with the newly created virus strains demonstrated that all constructs are also functionally expressed in rat sensory neurons (data not shown).

(4) Because viruses are self-amplifying transneuronal tracers, propagation within the nervous system and labeling of higher order neurons is not accompanied with a decrease in marker protein expression. Consequently, a high sensitivity of detection can be achieved.

In recent years, native PrV-Bartha as well as marker protein–expressing variants have been used efficiently to define the organization of central nervous system (CNS) circuits after intracerebral (Jasmin *et al*. 1997; DeFalco *et al*. 2001; Krout *et al*. 2003; Willhite *et al*. 2006) or peripheral (Jansen *et al*. 1995, 1997; Smith *et al*. 2000; Billig *et al*. 2000; Cano *et al*. 2001; Irnaten *et al*. 2001; Horvath *et al*. 2003) injection. The newly generated FCIP-expressing viral vectors represent a powerful tool for combining fast-tract tracing with physiological analysis applicable in multiple methodological approaches, including slice or *in vivo* imaging studies. *In vivo* two-photon calcium imaging provides the opportunity to simultaneously monitor the activity in multiple components of neural circuits at a cellular resolution. For this approach, an expression of virally encoded FCIPs would render complicated bulk-loading techniques or time-consuming construction of transgenic animals largely unnecessary. Moreover, they provide the possibility to study synaptically connected neuronal circuits in a holistic approach. In the future, the generation of FCIP-expressing wild-type PrV recombinants will also allow anterograde neuronal tract tracing.

The results presented here demonstrate that virally encoded FCIPs can be functionally expressed in infected murine neurons, enabling the exploration of calcium level changes in infected cells. In conclusion, these newly generated FCIP-expressing viral strains represent a perfect tool for the functional exploration of different neuronal systems *in vivo* and *in vitro*.

Declaration of interest: The authors report no conflicts of interest. The authors alone are responsible for the content and writing of the paper.

References

Alenius S, Dinter Z, Oberg B (1978). Therapeutic effect of trisodium phosphonoformate on cutaneous herpesvirus infection in guinea pigs. *Antimicrob Agents Chemother* **14:** 408–413.

Baird GS, Zacharias DA, Tsien RY (1999). Circular permutation and receptor insertion within green fluorescent proteins. *Proc Natl Acad Sci U S A* **96:** 11241–11246.

Bartha A (1961). Experimental reduction of virulence of Aujeszkýs disease virus. *Mag Allatorv Lapja* **16:** 42–45.

Billig I, Foris JM, Enquist LW, Card JP, Yates BJ (2000). Definition of neuronal circuitry controlling the activity of phrenic and abdominal motoneurons in the ferret using recombinant strains of pseudorabies virus. *J Neurosci* **20:** 7446–7454.

Cano G, Sved AF, Rinaman L, Rabin BS, Card JP (2001). Characterization of the central nervous system innervation of the rat spleen using viral transneuronal tracing. *J Comp Neurol* **439:** 1–18.

Damann N, Rothermel M, Klupp BG, Mettenleiter TC, Hatt H, Wetzel CH (2006). Chemosensory properties of murine nasal and cutaneous trigeminal neurons identified by viral tracing. *BMC Neurosci* **7:** 46.

DeFalco J, Tomishima M, Liu H, Zhao C, Cai X, Marth JD, Enquist L, Friedman JM (2001). Virus-assisted mapping of neural inputs to a feeding center in the hypothalamus. *Science* **291:** 2608–2613.

Diez-Garcia J, Matsushita S, Mutoh H, Nakai J, Ohkura M, Yokoyama J, Dimitrov D, Knopfel T (2005). Activation of cerebellar parallel fibers monitored in transgenic mice expressing a fluorescent Ca2+ indicator protein. *Eur J Neurosci* **22:** 627–635.

Enquist LW (2002). Exploiting circuit-specific spread of pseudorabies virus in the central nervous system: insights to pathogenesis and circuit tracers. *J Infect Dis* **186(Suppl 2):** S209–S214.

Fiala A, Spall T, Diegelmann S, Eisermann B, Sachse S, Devaud JM, Buchner E, Galizia CG (2002). Genetically expressed cameleon in Drosophila melanogaster is used to visualize olfactory information in projection neurons. *Curr Biol* **12:** 1877–1884.

Griesbeck O, Baird GS, Campbell RE, Zacharias DA, Tsien RY (2001). Reducing the environmental sensitivity of yellow fluorescent protein. Mechanism and applications. *J Biol Chem* **276:** 29188–29194.

Hasan MT, Friedrich RW, Euler T, Larkum ME, Giese G, Both M, Duebel J, Waters J, Bujard H, Griesbeck O, Tsien RY, Nagai T, Miyawaki A, Denk W (2004). Functional fluorescent Ca2+ indicator proteins in transgenic mice under TET control. *PLoS Biol* **2:** e163.

Helgstrand E, Eriksson B, Johansson N.G, Lannero B, Larsson A, Misiorny A, Noren JO, Sjoberg B, Stenberg K, Stening G, Stridh S, Oberg B (1978). Trisodium phosphonoformate: a new antiviral compound. *Science* **201:** 819–821.

Higashijima S, Masino MA, Mandel G, Fetcho JR (2003). Imaging neuronal activity during zebrafish behavior with a genetically encoded calcium indicator. *J Neurophysiol* **90:** 3986–3997.

Horvath M, Ribari O, Repassy G, Toth IE, Boldogkoi Z, Palkovits M (2003). Intracochlear injection of pseudorabies virus labels descending auditory and monoaminerg projections to olivocochlear cells in guinea pig. *Eur J Neurosci* **18:** 1439–1447.

Irnaten M, Neff RA, Wang J, Loewy AD, Mettenleiter TC, Mendelowitz D (2001). Activity of cardiorespiratory networks revealed by transsynaptic virus expressing GFP. *J Neurophysiol* **85:** 435–438.

Jansen AS, Hoffman JL, Loewy AD (1997). CNS sites involved in sympathetic and parasympathetic control of the pancreas: a viral tracing study. *Brain Res* **766:** 29–38.

Jansen AS, Nguyen XV, Karpitskiy V, Mettenleiter TC, Loewy AD (1995). Central command neurons of the sympathetic nervous system: basis of the fight-or-flight response. *Science* **270:** 644–646.

Jasmin L, Burkey AR, Card JP, Basbaum AI (1997). Transneuronal labeling of a nociceptive pathway: the spino-(trigemino-)parabrachio-amygdaloid: in the rat. *J Neurosci* **17:** 3751–3765.

Ji G, Feldman ME, Deng KY, Greene KS, Wilson J, Lee JC, Johnston RC, Rishniw M, Tallini Y, Zhang J, Wier W.G, Blaustein M.P, Xin H.B, Nakai J, Kotlikoff MI (2004). Ca2+-sensing transgenic mice: postsynaptic signaling in smooth muscle. *J Biol Chem* **279:** 21461–21468.

Kerr R, Lev-Ram V, Baird G, Vincent P, Tsien RY, Schafer WR (2000). Optical imaging of calcium transients in neurons and pharyngeal muscle of C. elegans. *Neuron* **26:** 583–594.

Krout KE, Mettenleiter TC, Loewy AD (2003). Single CNS neurons link both central motor and cardiosympathetic systems: a double-virus tracing study. *Neuroscience* **118:** 853–866.

Liu L, Yermolaieva O, Johnson WA, Abboud FM, Welsh MJ (2003). Identification and function of thermosensory neurons in Drosophila larvae. *Nat Neurosci* **6:** 267–273.

McCarthy KM, Tank DW, Enquist LW (2007). The effects of herpesvirus infection on neuronal excitability. In: Society for Neuroscience (SfN) Annual Meeting, November 3-7, 2007, San Diego, California, USA. Poster Abstracts, 697.27/R9.

Meyer zum Alten Borgloh S, Yang Y, Astori S, Zhu P, Migala A, Nagai T, Miyawaki A, Mank M, Griesbeck O, Palmer A. E, Tsien R.Y, Nakai J, Denk W, Sprengel R, Hasan MT (2006). Functional fluorescent calcium indicator proteins targeted to neurons using adeno-associated viral expression systems. In: Society for Neuroscience (SfN) Annual Meeting, October 14–18, Atlanta, Georgia, USA Poster Abstracts, 200.4/PP1.

Nagai T, Sawano A, Park ES, Miyawaki A (2001). Circularly permuted green fluorescent proteins engineered to sense Ca^{2+}. *Proc Natl Acad Sci U S A* **98:** 3197–3202.

Nakai J, Ohkura M, Imoto K (2001). A high signal-to-noise $Ca^{(2+)}$ probe composed of a single green fluorescent protein. *Nat Biotechnol* **19:** 137–141.

Reiff DF, Thiel PR, Schuster CM (2002). Differential regulation of active zone density during long-term strengthening of Drosophila neuromuscular junctions. *J Neurosci* **22:** 9399–9409.

Rothermel M, Schobel N, Damann N, Klupp BG, Mettenleiter TC, Hatt H, Wetzel CH (2007). Anterograde transsynaptic tracing in the murine somatosensory system using Pseudorabies virus (PrV): a "live-cell"-tracing tool for analysis of identified neurons in vitro. *J NeuroVirol* **13:** 579–585.

Smith BN, Banfield BW, Smeraski CA, Wilcox CL, Dudek FE, Enquist LW, Pickard GE (2000). Pseudorabies virus expressing enhanced green fluorescent protein: a tool for in vitro electrophysiological analysis of transsynaptically labeled neurons in identified central nervous system circuits. *Proc Natl Acad Sci U S A* **97:** 9264–9269.

Spehr J, Spehr M, Hatt H, Wetzel CH (2004). Subunit-specific P2X-receptor expression defines chemosensory properties of trigeminal neurons. *Eur J Neurosci* **19:** 2497–2510.

Suzuki H, Kerr R, Bianchi L, Frokjaer-Jensen C, Slone D, Xue J, Gerstbrein B, Driscoll M, Schafer WR (2003). In vivo imaging of C. elegans mechanosensory neurons demonstrates a specific role for the MEC-4 channel in the process of gentle touch sensation. *Neuron* **39:** 1005–1017.

Tallini YN, Ohkura M, Choi BR, Ji G, Imoto K, Doran R, Lee J, Plan P, Wilson J, Xin HB, Sanbe A, Gulick J, Mathai J, Robbins J, Salama G, Nakai J, Kotlikoff MI (2006). Imaging cellular signals in the heart in vivo: cardiac expression of the high-signal Ca^{2+} indicator GCaMP2. *Proc Natl Acad Sci U S A* **103:** 4753–4758.

Wang JW, Wong AM, Flores J, Vosshall LB, Axel R (2003). Two-photon calcium imaging reveals an odor-evoked map of activity in the fly brain. *Cell* **112:** 271–282.

Willhite DC, Nguyen KT, Masurkar AV, Greer CA, Shepherd GM, Chen WR (2006). Viral tracing identifies distributed columnar organization in the olfactory bulb. *Proc Natl Acad Sci U S A* **103:** 12592–12597.

Yu D, Baird GS, Tsien RY, Davis RL (2003). Detection of calcium transients in Drosophila mushroom body neurons with camgaroo reporters. *J Neurosci* **23:** 64–72.